Bifurcations in the attitude dynamics of a spacecraft in a gravity field

M. Arribas[a,*], D. Casanova[a], A. Elipe[a,b], M. Palacios[a]

[a] *Grupo de Mecánica Espacial-IUMA. Universidad de Zaragoza. Spain*
[b] *Centro Universitario de la Defensa de Zaragoza. Spain*

Abstract

In the problem of the attitude dynamics of a rigid body satellite in a gravity field, in the averaged Hamiltonian the global parametric evolution of the normalized Hamiltonian is obtained. The phase portrait is represented in a Mercator map and on a 3D sphere. Pitch-fork bifurcations and degeneracies (a dense set of equilibria) are found.

Keywords: Attitude dynamics, Rigid body motion, Bifurcations

1. Introduction

Attitude dynamics of a rigid body is a classic problem in Mechanics that has been studied by the most famous scientists. In this context, we find names like Newton, Euler, Lagrange, Laplace, Poinsot, Poisson, Hamilton, Cayley, Kowaleskaya, Liapunov, etc. (see e.g. Leimanis' textbook (Leimanis, 1965)).

The so-called Euler-Poinsot problem (rigid body in free rotation) is one of the three integrable problems in the rigid-body dynamics, and it is very interesting for both practical and theoretical point of view. It is related with important astronomical problems like the rotation of planets, satellites, asteroids, etc. and also with astrodynamics, since a good knowledge of the attitude of spinning spacecraft is essential in designing a mission.

Gravitational torques are fundamental to the attitude dynamics of a spacecraft, and their influence on the rotational motion of an artificial satellite have been studied in the last years (see e.g. Hughes (1986); Arribas and Elipe (1993); Elipe and Vallejo (2001); Elipe (2002)). In order to maintain alive a mission, it is essential the stability analysis of the rotational motion (Pavlov and Maciejewski, 2003; Sarychev et al., 2007, 2008; de Moraes et al., 2009), since the choice of a set of wrong initial conditions could put the spacecraft in tumbling rotation, leading to a chaotic regime and ruining the mission.

On the other hand, some substantial progress has been made in the understanding of small perturbations of integrable systems. After the KAM theory, it is known that invariant tori in the unperturbed problem are slighted distorted in presence of small perturbations, with presence of periodic orbits lying on these tori, while for larger perturbations part of the tori are destroyed, and chaotic orbits appear filling the so-called regions of stochasticity.

To determine regular and chaotic regions, as well as periodic and quasi-periodic solutions in two degrees of freedom, Poincaré surface of sections are widely used. The rigid body dynamics is not an

*Corresponding author
Email address: marribas@unizar.es (M. Arribas)

exception, and thus, we find the work of Broucke (1993), for instance. A more modern technique like the use of Chaos indicators have been employed to determine chaotic regions in the motion of a rigid body under external torques (Barrio et al., 2006). However, in this work, we proceed in a different way. Indeed, by means of averaging or normalization, the original non-integrable Hamiltonian is replaced by an integrable approximation that is built to give a good agreement with real dynamics. Of particular importance in this problem is the qualitative analysis of the equations of the motion, in order to know, before integrating the equations, how the phase flow varies according to the initial conditions, what are the stability regions, whether there are bifurcations, and for what values of the initial conditions they occur (Lanchares and Elipe, 1995a,b). Let us remind that parametric bifurcations are the seeds of chaos.

In the present paper, we assume that the Earth possesses a spherically symmetry mass distribution, that the spacecraft is small compared to its distance from the mass center of the primary, and that the spacecraft consists of a rigid body with three different moments of inertia. However for the sake of simplicity, the qualitative analysis is done for the case of axial symmetry. The Hamiltonian is formulated in polar–nodal variables to describe the orbit of the center of mass, and in Serret–Andoyer for the attitude motion.

2. Hamiltonian of the Problem

Let us consider the problem of the rotational–translational motion of a rigid body (the spacecraft) attracted by the gravity field of the Earth (a point mass). In the literature, this problem has been formulated in terms of Delaunay variables to describe the orbital motion and in Serret–Andoyer for the attitude (Kinoshita, 1972; Arribas and Elipe, 1993).

The use of Delaunay variables involves developments of powers of the inverse of the radius vector in terms of the eccentricity. However, this inconvenience may be avoided by employing the polar–nodal variables (r, θ, ν, R, Θ, N).

First at all, we have to choose an appropriate set of reference frames, in order to obtain a simpler formulation. We consider the following frames centered on the spacecraft:

- A fixed space frame $O\boldsymbol{s}_1\boldsymbol{s}_2\boldsymbol{s}_3$.
- The system $O\ell_0 m_0 n$, where n is the unit vector in the direction of the rotational angular momentum G and ℓ_0 is the ascending node of the plane perpendicular to the vector $\boldsymbol{G}$ and the space plane $O\boldsymbol{s}_1\boldsymbol{s}_2$.
- The principal body frame of inertia $O\boldsymbol{b}_1\boldsymbol{b}_2\boldsymbol{b}_3$.

The Serret–Andoyer variables (ℓ, g, h, L, G, H) are defined as usual (Deprit, 1967; Deprit and Elipe, 1993):
The angle h is the longitude of the ascending node $\boldsymbol{\ell}_0$ reckoned from the axis $\boldsymbol{s}_1$; g is the longitude of the node $\boldsymbol{\ell}_1$ of the equatorial body plane $O\boldsymbol{b}_1\boldsymbol{b}_2$ on the plane perpendicular to the angular momentum reckoned from the axis $\boldsymbol{\ell}_0$; ℓ is the longitude of the body axis $\boldsymbol{b}_1$ reckoned from the node $\boldsymbol{\ell}_1$.
The conjugate moments are: $G = \|\boldsymbol{G}\|$, the norm of the rotation angular momentum vector, H,the projection of this vector on the space axis $\boldsymbol{s}_3$, ($H = G\cos\epsilon$), and finally, L is the projection of $\boldsymbol{G}$ on the body axis b_3, ($L = G\cos\sigma$). The Hamiltonian function of the problem, considering only

terms up to the third power of the inverse of the distance, and after some simplifications may be written as Arribas and Elipe (1993)

$$\mathcal{H} = \mathcal{H}_K + \mathcal{H}_E + \mathcal{H}_C \tag{1}$$

where

$$\begin{aligned}
\mathcal{H}_K &= \frac{1}{2}(R^2 + \frac{\Theta^2}{r^2}) - \frac{\mu}{r}, \\
\mathcal{H}_E &= \left(\frac{\sin^2\ell}{2I_1} + \frac{\cos^2\ell}{2I_2}\right)(G^2 - L^2) + \frac{1}{2I_3}L^2, \\
\mathcal{H}_C &= -\frac{\mu}{2r^3}\Big[(I_1 - I_2)(1 - 3\alpha^2) + (I_3 - I_2)(1 - 3\gamma^2),\Big]
\end{aligned}$$

and I_1, I_2, I_3 are the principal moments of inertia of the satellite (which we shall assume $I_1 \leq I_2 \leq I_3$), (α, β, γ) is the unit vector in the radial direction in the body frame.

The two nodes, the orbital ν and the rotational one h, are on the same plane ($O\boldsymbol{s}_1\boldsymbol{s}_2$), and in the development of the potential function, they appear only as the combination $h - \nu$. Besides, in the problem of motion given by the Hamiltonian (1), the total angular momentum vector $\boldsymbol{c}$, is an integral of the motion, and this allows us to choose the space frame in such a way that the axis $\boldsymbol{s}_3$ coincides with this vector. (For more details, see Arribas (1989); Breiter and Elipe (2006)).

With this election, and $\boldsymbol{\Theta}$ and $\boldsymbol{G}$ standing for the orbital and rotational angular moments respectively, in the space frame we have

$$\boldsymbol{\Theta} + \boldsymbol{G} = \boldsymbol{c} = (0, 0, c) \quad \text{with} \quad c = \text{constant}, \tag{2}$$

and the nodes satisfy the relation $h - \nu = \pi$. The angles h and ν being cyclic, the problem has four degrees of freedom in the variables (r, θ, ℓ, g, R, Θ, L, G).

Let us assume that the Hamiltonian (1) may be decomposed as

$$\mathcal{H} = \mathcal{H}_0 + \mathcal{H}_1,$$

where the zero order term is formed by the Keplerian and Eulerian parts $\mathcal{H}_K$ and $\mathcal{H}_E$, whereas the coupled terms ($\mathcal{H}_C$) are of order one.

We are not interested in obtaining the solution of this Hamiltonian, but we content ourselves with studying the qualitative analysis of an averaged Hamiltonian of (1) in order to discovered the behavior of the phase flow and possible bifurcations for different values of the initial conditions. Furthermore, we shall make a simplification by averaging the Hamiltonian over the Keplerian mean anomaly.

After performing automatically this average and dropping those terms which do not contain the variables, we obtain:

$$\begin{aligned}
\mathcal{H}^* = \quad & \left(\frac{\sin^2\ell}{2I_1} + \frac{\cos^2\ell}{2I_2}\right)(G^2 - L^2) + \frac{1}{2I_3}L^2 \\
& -\frac{\mu n}{2\Theta p}\Big[(I_1 - I_2)(1 - 3\alpha^{*2}) + (I_3 - I_2)(1 - 3\gamma^{*2})\Big]
\end{aligned} \tag{3}$$

where n is the orbital mean motion, p is the semilatus rectus, and

$$\begin{aligned}
\alpha^{*2} &= A_0 + A_1\cos g + A_2\cos 2g + A_3\cos 2\ell + A_4\cos(g + 2\ell) \\
&\quad + A_5\cos(g - 2\ell) + A_6\cos(2g + 2\ell) + A_7\cos(2g - 2\ell),
\end{aligned} \tag{4}$$

$$\gamma^{*2} = G_0 + G_1\cos g + G_2\cos 2g,$$

with the coefficients A_i and G_i being expressions which depend on the moments Θ, N, L, G, H (see e.g. (Arribas, 1989)).

3. Qualitative analysis of the phase flow

3.1. Definition of variables and parameters

The zero order of the Hamiltonian (3) corresponds to the rotation of a tri-axial rigid body in free rotation, it is one-degree of freedom problem, and is integrable in terms of elliptic functions (Deprit and Elipe, 1993); therefore, it is possible to build a Lie-transformation in order to elliminate the variable ℓ form the Hamiltonian (3), see (Arribas and Elipe, 1993; Elipe and Vallejo, 2001, e.g.). However for the sake of simplicity, we shall consider the case in which the satellite has axial symmetry of inertia, i.e., $I_1 = I_2$. Under this hypothesis, the variable ℓ becomes cyclic, and the Hamiltonian is reduced to:

$$\begin{aligned}\mathcal{H}^* &= \frac{1}{2I_1}(G^2 - L^2) + \frac{1}{2I_3}L^2 \\ &\quad -\frac{\mu n}{2\Theta a(1-e^2)}(I_3 - I_1)\,\left[1 - 3\left(G_0 + G_1\cos g + G_2\cos 2g\right)\right]\end{aligned}$$

which exclusively depends on g and G and where n stands for the orbital mean motion, a is the semi major axis and e the orbital eccentricity. The averaged problem is of one-degree of freedom and therefore, it is integrable.

The zero-order of the above Hamiltonian corresponds to the rotation of an axis-symmetric rigid body, and it is well known that its motion consists of rotations about the axis of symmetry, thus, we will take into consideration only the perturbation.

The behavior of the flow corresponding to the perturbed part is the same as in

$$\mathcal{K} = G_0 + G_1\cos g + G_2\cos 2g, \tag{5}$$

where G_0, G_1, G_2 are

$$\begin{aligned}G_0 &= \tfrac{1}{2}\sin^2\epsilon\cos^2\sigma + \tfrac{1}{4}(1+\cos^2\epsilon)\sin^2\sigma,\\ G_1 &= \sin\epsilon\cos\epsilon\sin\sigma\cos\sigma,\\ G_2 &= \tfrac{1}{4}(\cos^2\epsilon\sin^2\sigma - \sin^2\epsilon),\end{aligned}$$

which result after dropping constant terms and scaling the problem.

In order to make a qualitative analysis of the phase flow of this Hamiltonian, it is convenient to choose a parameter. Having in mind that the inclination angles σ and ϵ are given in terms of the moments L, G, H by

$$\cos\sigma = \frac{L}{G}, \qquad \cos\epsilon = \frac{H}{G};$$

they are related by $\cos\sigma = (L/H)\cos\epsilon$, with L/H constant; so, we choose $p = L/H$ as a parameter. In order to handle polynomial expressions, which is easier than handling trigonometric functions, we make the change

$$\eta = \cos\epsilon, \quad \text{where} \quad |\eta| \le \widehat{\eta} = \min\{1, 1/p\},$$

and thus, the Hamiltonian is expressed as

$$\begin{aligned}\mathcal{K} &= \tfrac{1}{2}p^2\eta^2(1-\eta^2) + \tfrac{1}{4}(1+\eta^2)(1-p^2\eta^2)\\ &\quad + p\eta^2\sqrt{1-p^2\eta^2}\sqrt{1-\eta^2}\cos g + \tfrac{1}{4}(2\eta^2 - 1 - p^2\eta^4)\cos 2g,\end{aligned} \tag{6}$$

with the coordinates $(g,\eta)\in[0,2\pi)\times[-\widehat{\eta},\widehat{\eta}]$.

At this point, let us note that the above expression of Hamiltonian (6) has some symmetries. Indeed, there are two lines of symmetry, namely, the axis $\eta=0$ since $\mathcal{K}(g,\eta;p)=\mathcal{K}(g,-\eta;p)$ and the the line $g=\pi$, since $\mathcal{K}(\pi-g,\eta;p)=\mathcal{K}(\pi+g,\eta;p)$. With this, we may restrict our analysis to the region $(g,\eta)\in[0,\pi]\times[0,\widehat{\eta}]$. Besides, since $\mathcal{K}(g,\eta;p)=\mathcal{K}(g\pm\pi,\eta;-p)$, we reduce our analysis to $p\geq 0$.

3.2. Analytical study

Equilibria are obtained by zeroing simultaneously the derivatives dg/dt and dG/dt. That is, by solving the system

$$\frac{dg}{dt}=\frac{\partial\mathcal{K}}{\partial G}=\frac{\partial\mathcal{K}}{\partial\eta}\frac{\partial\eta}{\partial G}=\frac{-H}{G^2}\left(\frac{\partial G_0}{\partial\eta}+\frac{\partial G_1}{\partial\eta}\cos g+\frac{\partial G_2}{\partial\eta}\cos 2g\right)=0, \tag{7}$$

$$\frac{dG}{dt}=-\frac{\partial\mathcal{K}}{\partial g}=(G_1+4G_2\cos g)\sin g=0. \tag{8}$$

This system is complex enough and some numerical procedure is required to solve it. However, there are particular cases which solution is easy to find.

First at all, let us compute the main term in (7). After some algebra, we have

$$\left(\frac{\partial G_0}{\partial\eta}+\frac{\partial G_1}{\partial\eta}\cos g+\frac{\partial G_2}{\partial\eta}\cos 2g\right)=$$
$$-\frac{1}{2}\eta(6\eta^2p^2-1-p^2)+\frac{\eta p(2-3(1+p^2)\eta^2+4p^2\eta^4)}{\sqrt{1-\eta^2}\sqrt{1-p^2\eta^2}}\cos g+\eta(1-p^2\eta^2)\cos 2g.$$

The second equation (8) is

$$(G_1+4G_2\cos g)\sin g=\left(p\eta^2\sqrt{1-\eta^2}\sqrt{1-p^2\eta^2})+(-1+2\eta^2-p^2\eta^4)\cos g\right)\sin g.$$

If $H=0$, because its definition, $\eta=0$, and hence, the first equation (7) of the system is always null. Besides, the second equation is reduced to $\sin 2g=0$, which satisfied for $g=k\pi/2$ ($k\in\mathbb{Z}$). That is, since our analysis is reduced to the interval $g\in[0,\pi]$, the points $(0,0)$, $(0,\pi/2)$, and $(0,\pi)$ are equilibria.

Let us assume now that $H\neq 0$ ($\eta\neq 0$), then we have to cases:

1. The second equation (8) is satisfied for $g=k\pi$ ($k\in\mathbb{Z}$). Then, the first equation (7) for $g=k\pi$ becomes

   $$\frac{\partial G_0}{\partial\eta}\pm\frac{\partial G_1}{\partial\eta}+\frac{\partial G_2}{\partial\eta}=0,$$

   depending on either $g=0$ (+) or $g=\pi$ (−), or explicitly,

   $$\eta\quad\frac{1}{2}(3+p^2-8p^2\eta^2)\pm\frac{p(2-3(1+p^2)\eta^2+4p^2\eta^4)}{\sqrt{1-\eta^2}\sqrt{1-p^2\eta^2}}\right)=0.$$

   When $p=1$ and $g=\pi$, the expression $\partial(G_0-G_1+G_2)/\partial\eta\equiv 0$ for whatever value of $\eta\in[-1,1]$. Thus, for $p=1$, the segment (π,η) is made of equilibria; hence, we are in presence of a degeneracy.

2. Assume now that $\sin g \neq 0$, then the second equation (8) holds when

$$G_1 + 4G_2 \cos g = 0 \tag{9}$$

Besides, let us take the particular case $p = 1$; then the above equation (9) becomes $\eta^2 + (1 - \eta^2)\cos g = 0$, that is,

$$\eta = \sqrt{\frac{\cos g}{1 + \cos g}}. \tag{10}$$

If we replace this value of η into the first equation of the system (7), it is always satisfied for whatever value of g. Hence, we meet another degeneracy for $p = 1$. Every point on the curve (10) is an equilibrium of the system.

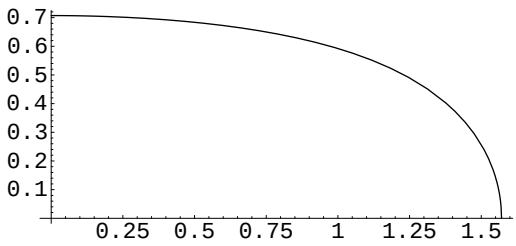

Figure 1: For $p = 1$, all points (g, η) of this curve, Eq. (10), are of equilibria.

Let us consider now that $g \neq 0, \pi$, then the equation (8) is fulfilled for

$$\cos g = -G_1/(4G_2). \tag{11}$$

If we replace it into equation (7), the possible equilibria will result by solving the equation

$$\frac{\partial G_0}{\partial \eta} - \frac{\partial G_1}{\partial \eta}\frac{G_1}{4G_2} + \frac{\partial G_2}{\partial \eta}\left(\frac{G_1^2}{8G_2^2} - 1\right) = 0,$$

which in terms of η, is

$$\frac{\eta(1-p^2)(-1 + 4\eta^2 + -4(1-p^2)\eta^4 - 4p^2\eta^6 + p^4\eta^8)}{2(1 - 2\eta^2 + p^2\eta^4)^2} = 0,$$

or equivalently,

$$-1 + 4\eta^2 + -4(1-p^2)\eta^4 - 4p^2\eta^6 + p^4\eta^8 = 0, \tag{12}$$

since the cases $\eta = 0$ and $p = 1$ have been already studied.

For each value of the parameter p we have to solve the above equation (12), to obtain η and with it we get the angle g from Eq. (11).

The above equation can be put as

$$-1 + 4\xi + -4(1-p^2)\xi^2 - 4p^2\xi^3 + p^4\xi^4 = 0, \quad \text{with} \quad \eta^2 = \xi,$$

easier to solve numerically, and we only need those solutions $0 < \xi < 1$.

3.3. Stability and bifurcations

Now, we are interested in finding analytically the values of the parameter for which the bifurcations occur. So, we have to obtain the characteristic equation for the differential system.

By means of Liouville theorem, we have

$$\frac{d\eta}{dt} = \{\eta, \mathcal{K}\} = -\frac{\partial \eta}{\partial G}\frac{\partial \mathcal{K}}{\partial g}$$

where $\{\ ,\ \}$ stands for the Poisson bracket.

After a time scaling $t \longmapsto \tau$ given by the relation

$$d\tau = \frac{\partial \eta}{\partial G}\, dt,$$

the variational equations of the motion in an equilibrium point are

$$\frac{d\,\delta g}{d\,\tau} = A\,\delta\eta + B\,\delta g \qquad \frac{d\,\delta\eta}{d\,\tau} = -C\,\delta\eta - D\,\delta g$$

$$\frac{d}{d\,\tau}\begin{pmatrix} \delta g \\ \delta\eta \end{pmatrix} = \begin{pmatrix} B & A \\ -D & -C \end{pmatrix}\begin{pmatrix} \delta g \\ \delta\eta \end{pmatrix}$$

where

$$A = \frac{\partial^2 \mathcal{K}}{\partial \eta^2},\ B = \frac{\partial^2 \mathcal{K}}{\partial \eta \partial g} = C,\ D = \frac{\partial^2 \mathcal{K}}{\partial g^2}.$$

The associated characteristic polynomial equation is $\lambda^2 + (AD - B^2) = 0$ and therefore, an equilibrium point is unstable when $(AD - B^2) < 0$.

Let us consider some of the equilibria just obtained. For the point $(\pi, 0)$, the characteristic polynomial becomes

$$\lambda^2 + (AD - B^2) = \lambda^2 + \tfrac{1}{2}(3 - 4p + p^2),$$

thus, this point will be unstable when $3 - 4p + p^2 < 0$, that is, when $p \in (1, 3)$. The bifurcations (that is change of stability) occur in the extrema of it, that is to say, for $p = 1$ and for $p = 3$. In fact, these two values are the bifurcation values of p as portrayed in the phase space graphics.

For the point $(\pi/2, 0)$, the characteristic polynomial becomes

$$\lambda^2 + (AD - B^2) = \lambda^2 + \frac{1}{2}(1 - p^2),$$

hence, this point is stable for $p \in [0, 1)$ and unstable for $p > 1$. The bifurcation occurs at $p = 1$.

For the origin, the discriminant $\Delta = (AD - B^2) = (3 - 4p + p^2)/2$ is positive for $p > 0$, which means that is always stable in the studied interval and therefore, if does not bifurcate.

The sign of the discriminant may be used to determine the stability of whatever equilibrium. Thus, for instance, in the next section, we find that the point $(1.169863462, 0.546038088)$ is stationary for $p = 0.8$. Replacing the point and the parameter in the discriminant, we find that $\Delta = -0.49427$, thus, is unstable.

4. Graphical analysis. Mercator maps

In order to understand how, qualitatively speaking, the phase flow varies with the parameter p, one should first determine the equilibria. This kind of analysis is often very ackward. But we are greatly assisted if we can generate at will portraits of the phase flow for any value of the parameter.

In the plots of this section, we present the phase portrait on the Mercator chart (g, η). We consider $p \in [0, 3.1]$, since the qualitative behavior of the phase flow does not change for $p > 3$.

Let us start with $p = 3.1$; the phase flow is represented in Figure 2. In fact, and due to the symmetries previously mentioned, the phase portrait is a cylinder, and because of the symmetry about the line $g = \pi$, we only need the interval $0 \leq g \leq \pi$. On the left plot, and for $\eta = 0$ we can see three equilibria at $g = 0, \pi/2, \pi$. Point $(\pi/2, 0)$ is unstable whereas the other two $(0, 0)$ and $(\pi, 0)$ are stable. Besides, the point $(0, 0.290432785)$ is an unstable equilibrium (see Fig. 2).

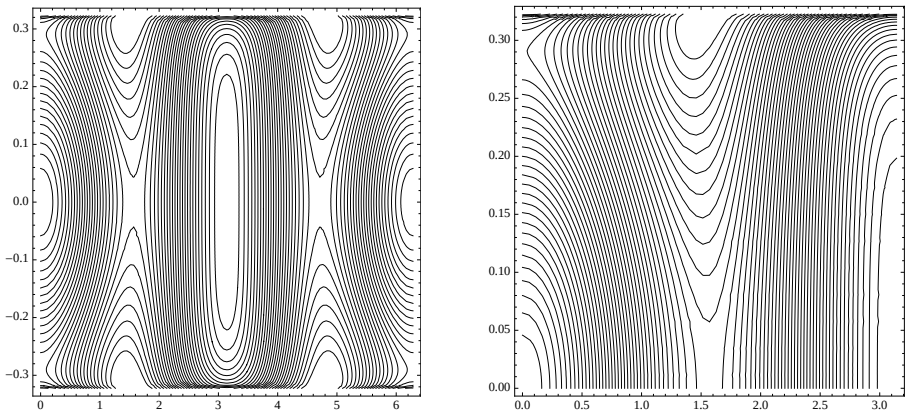

Figure 2: Level contours for $p = 3.1$. Left, in the domain $(g, \eta) \in [0, 2\pi) \times (-1/p, 1/p)$. Right, in the domain $(g, \eta) \in [0, \pi) \times [0, 1/p)$.

For $p = 3$ there is a pitch-fork bifurcation at the point $(\pi, 0)$. Indeed, as we can observe in Fig. 2, for $p \geq 3$ is stable; however, for $p < 3$, this point is unstable and there is one new stable point (Fig. 3) on the vertical axis $\eta = \pi$, inside the homoclinic orbit that springs out from the point $(\pi, 0)$.

Let us analyze the phase flow after the pitchfork bifurcation, that is, for $p < 3$; for example for $p = 2$ (see Fig. 3). In the phase rectangle $(g, \eta) \in [0, \pi] \times [0, 1/2)$, we find six equilibria, three stable $(0, 0)$, $(1.343527124,\ 0.418877566)$ and $(\pi, 0.29653517)$, and other three unstable, namely, the points $(\pi/2, 0)$, $(\pi, 0)$ and $(0, 0.42153516)$.

The flow is qualitatively the same until we reach the value $p = 1$, where there are two degeneracies, as we already proved in the above section. The first one is the line $g = \pi$, which is a dense set of equilibria; indeed, as $p \to 1$, the homoclinic orbit emanating at the point $(\pi, 0)$, narrows until it collapses into the straight line $g = \pi$, which is made of equilibria (Fig. 4). As soon as $p < 1$, the degenerary breaks out and only two equilibrium points remain, the stable $(\pi, 0)$ and another one unstable. For $p = 0.8$, this unstable equilibrium is $(2.413433567, 0.922181580)$.

Simultaneously, another degeneracy happens; the heteroclinic orbit connecting unstable points on the axis $g = 0$ coalesces as $p \to 1$ with the homoclinic orbit emanating from $(\pi/2, 0)$ and the resulting line is made of equilibria. As soon as $p < 1$, this degeneracy breaks out, and there are three new equilibria, one unstable and two stable (Fig. 4). For $p = 0.8$, these points are: the unstable $(1.169863462, 0.546038088)$ and the stable $(0, 0.800834940)$, $(\pi/2, 0)$.

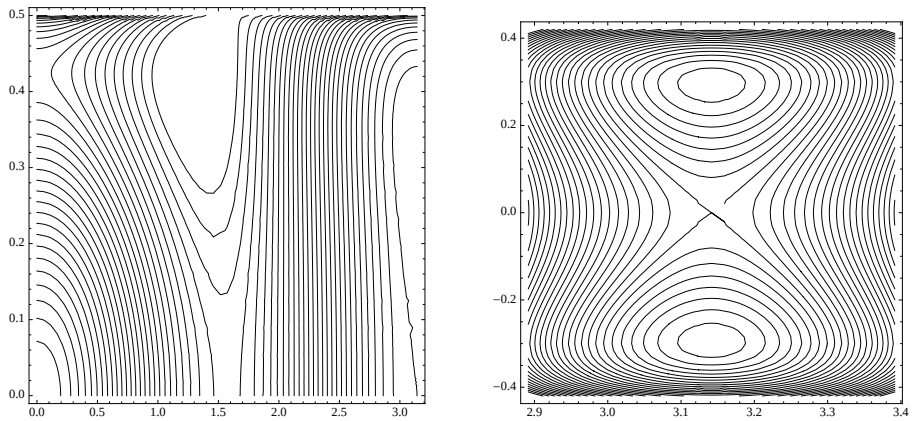

Figure 3: Phase flow for $p = 2.0$. Left, we can see three unstable points and three stable equilibria in the rectangle $(g, \eta) \in [0, \pi] \times [0, 1/2)$. Right, a magnification of the neighborhood of $g = \pi$.

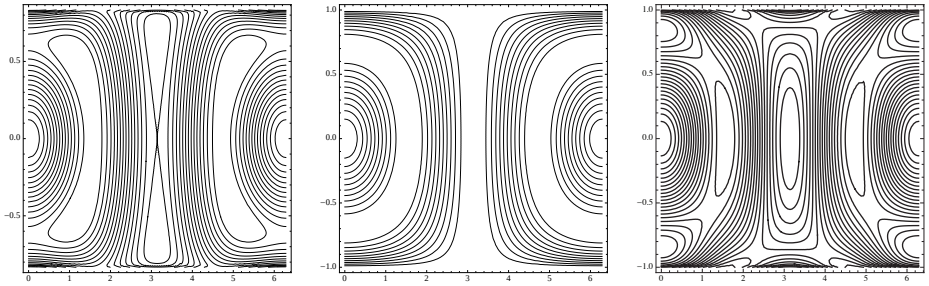

Figure 4: Evolution of the fhase flow through two simultaneous degeneracies at $p = 1$. Left) flow for $p = 1.2$; center) flow for $p = 1.$; and right) flow for $p = 0.8$.

In sum, for $0 \leq p < 1$, in the phase rectangle $(g, \eta) \in [0, \pi] \times [0, 1/2)$, there are six equilibria (Fig. 4, right), four stable and two unstable.

5. Graphical analysis. Spheres

As we just showed, the Mercator maps reveals to be very efficient for determining the equilibria and the different bifurcations, however, as it is usual with this representation (Coffey et al., 1990), it gives no information on the upper and lower limits of the chart, that is, on the lines $|\eta| = \widehat{\eta}$. To circumvent this problem we shall use a set of spherical coordinates, since as we prove, the flow lies on spheres.

Let us define the dimensionless quantities:

$$\xi_1 = \frac{L}{H}\sqrt{1 - \frac{H^2}{G^2}}\cos g, \quad \xi_2 = \frac{L}{H}\sqrt{1 - \frac{H^2}{G^2}}\sin g, \quad \xi_3 = \frac{L}{G}; \tag{13}$$

they are not algebraically independent, but they are related by

$$\xi_1^2 + \xi_2^2 + \xi_3^2 = L^2/H^2 = p^2, \tag{14}$$

thus, the above equation represents a two-dimensional sphere of constant radius p.

The Hamiltonian (6) expressed in these spherical variables is

$$\begin{aligned}\mathcal{K} &= \frac{1}{2p^2}\xi_3^2(\xi_1^2+\xi_2^2)+\frac{1}{p^2}\xi_1\xi_3^2\sqrt{1-\xi_3^2}+\frac{1}{4}(1-\xi_3^2)\left(1+\frac{\xi_3^2}{p^2}\right)+\\ &+\frac{1}{4p^2}\frac{\xi_1^2-\xi_2^2}{\xi_1^2+\xi_2^2}\left(\xi_3^2(1-\xi_3^2)-(p^2-\xi_3^2)\right).\end{aligned} \tag{15}$$

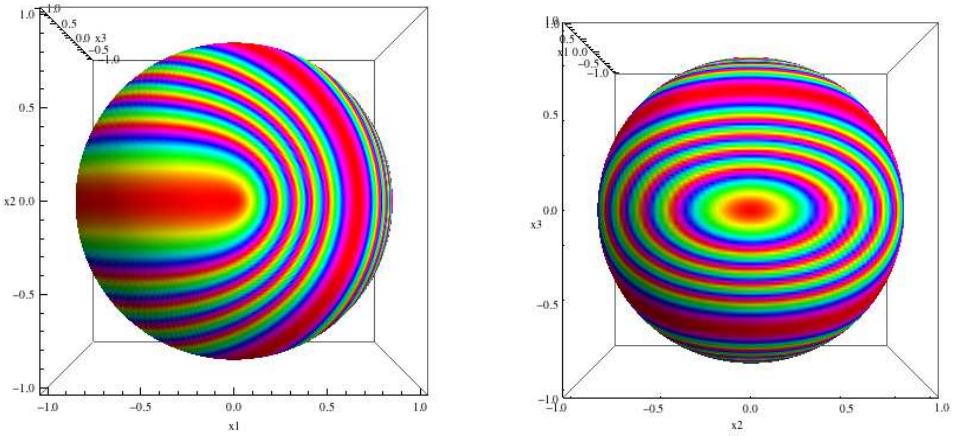

Figure 5: Phase portrait for $p = 1$. Left) view from the point (0,0,1), and right) view from the point (1,0,0). On the left plot we can appreciate two lines of degeneracy, namely the hemi-meridian ($\xi_2 = 0,\ \xi_1 \geq 0$) (which corresponds to the segment $g = 0$ in the Mercator map, and the curve on the sphere which corresponds to the curve on the Fig. 1. In the right plot we can see the latter curve of degeneracy as well as the stable point ($g = 0, \eta = 0$).

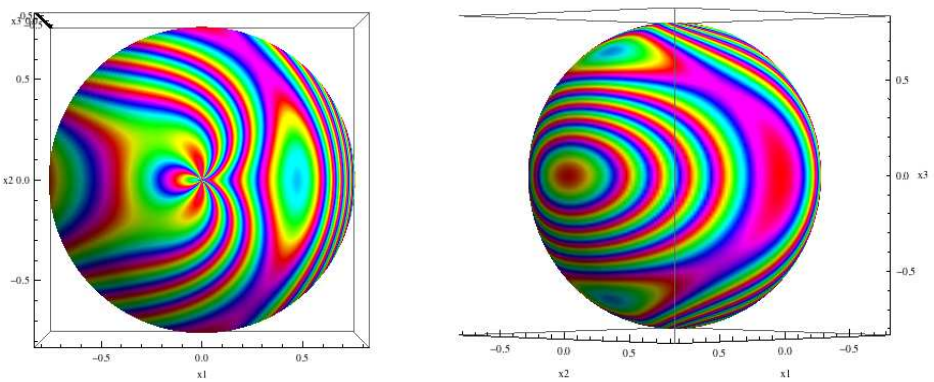

Figure 6: Phase portrait for $p = 0.8$. Left) view from the point (0,0,1), and right) view from the point (1,1,0). On the left plot, we can see how the upper line of Fig. 4,right) merges into a unique point, the north pole of the sphere. The right plot shows two unstable and four stable points which corresponds with the one we can see in Fig. 4, right).

The equations of motion generated by this Hamiltonian flow are

$$\dot{\xi}_j = \{\xi_j, \mathcal{K}\}, \qquad (j = 1, 2, 3),$$

which may be easily computed taking into account that the mutual Poisson brackets of coordinates

(13) are

$$\{\xi_1, \xi_2\} = \frac{1}{L}\,\xi_3^3, \quad \{\xi_2, \xi_3\} = \frac{1}{L}\,\xi_1\,\xi_3^2, \quad \{\xi_3, \xi_1\} = \frac{1}{L}\,\xi_2\,\xi_3^2.$$

In order to have the phase portrait of Hamiltonian (15), we could plot the trajectories by integrating numerically the above equations of motion for several values of the energy. However, we can proceed in a different way, with no use of the equations of motion. Indeed, we can visualize the phase flow by *painting the Hamiltonian* (Coffey et al., 1990). It is based on an orthograpic projection which maps the points on the phase space onto the screen of the computer; according to the values of the energy, a color is assigned to each point of the projection. Although this technique was elaborated for parallel computers to produce high resolution pictures, today can be produced with general software (Mathematica in our case). For instance, the plots of Figs. 5 and 6 were obtained with the simple Mathematica instruction:

```
ParametricPlot3D[
 {p Sin[sigma] Cos[g], p Sin[sigma] Sin[g], p Cos[sigma]}, {g, 0, 2 Pi},
 {sigma, 0, Pi}, Mesh -> False, ColorFunction -> Function[{x1, x2, x3},
 Hue[Hamiltonian]], PlotPoints -> 200, AxesLabel -> {"x1", "x2", "x3"},
 ColorFunctionScaling -> False, ViewPoint -> {10, 10, 0}]
```

Hence, by means of the snap shots for different values of p we have the parametric evolution of the phase flow, with no need on integrating the equations of motion.

6. Conclusions

The use of *visualization techniques* in 2D and 3D revealed to be very useful to analyze integrable Hamiltonian problems. Both techiques have been applied to the normalized Hamiltonian corresponding to the attitude of an axis-symmetric rigid body under a gravity field. For this problem, we found the bifurcations as well as two degenerate cases, that is, cases in which there are infinite equilibria.

Acknowledgments

Supported by the Spanish Ministry of Science and Innovation (Projects # AYA2008-05572 and # MTM2009-10767).

References

Arribas, M. (1989). *Sobre la dinámica de actitud de satélites artificiales.* PhD thesis, Universidad de Zaragoza.
Arribas, M. and Elipe, A. (1993). *Celest. Mech. Dyn. Astr.*, 55:243–247.
Barrio, R., Blesa, F., and Elipe, A. (2006). *J. Astronaut. Sci.*, 54:359–368.
Breiter, S. and Elipe, A. (2006). *Celest. Mech. Dyn. Astr.*, 95:287–297.
Broucke, R. (1993). *J. Astronaut. Sci.*, 41(4):593–601.
Celleti, A. and Voyatzis, G. (2010). *Celest. Mech. Dyn. Astr.*, 107:101–113.
Coffey, S., Deprit, A., Deprit, E., and Healy, L. (1990). *Science*, 247:769–892.
de Moraes, R., Cabette, R., Zanardi, M., Stuchi, T., and Formiga, J. (2009). *Celest. Mech. Dyn. Astr.*, 104:337–353.
Deprit, A. (1967). *Am. J. Phys.*, 35(5):424–428.
Deprit, A. and Elipe, A. (1993). *J. Astronaut. Sci.*, 41(4):603–628.
Elipe, A. (2002). *Int. J. Theor. Phys.*, 8:163–196.
Elipe, A. and Vallejo, M. (2001). *Celest. Mech. Dyn. Astr*, 8:3–12.
Hughes, P. C. (1986). *Spacecraft Attitude Dynamics.* John Wiley ans Sons, New York.

Kinoshita, H. (1972). *Publ. Astron. Soc. Jpn.*, 24:423–439.
Lanchares, V. and Elipe, A. (1995a). *Chaos*, 5:367–373.
Lanchares, V. and Elipe, A. (1995b). *Chaos*, 5:531–535.
Leimanis, E. (1965). *The General Problem of the Motion of Coupled Rigid Bodies about a Fixed Point*. Springer Verlag, Berlin.
Pavlov, A. and Maciejewski, A. (2003). *Astron. Lett.*, 29(8):552–566.
Sarychev, V., Mirer, S., Degtyarev, A., and Duarte, E. (2007). *Celest. Mech. Dyn. Astr.*, 97(4):267–287.
Sarychev, V., Mirer, S., and Degtyarev, A. (2008). *Celest. Mech. Dyn. Astr.*, 100(4):301–318.